

Electron Transfer between Reactants Located on Opposite Sides of Liquid/Liquid Interfaces

Chunnian Shi and Fred C. Anson*

*Arthur Amos Noyes Laboratories, Division of Chemistry and Chemical Engineering, California Institute of Technology, Pasadena, California 91125**Received: April 2, 1999; In Final Form: June 1, 1999*

A recently introduced method for interposing thin layers of organic solvents between graphite electrode surfaces and aqueous solutions was used to examine the effects of the nature and concentration of the supporting electrolytes on electrochemical responses for reactants dissolved in the thin layers of organic solvent. The method was also used to evaluate the rates of electron transfer between coreactants, each of which was confined to one of the two adjoining, immiscible phases. The rates of these electron-transfer reactions were shown not to be influenced by simultaneous cross-phase ion-transfer processes in cases where such processes were forced to proceed. The rates of the electron-transfer reactions exhibited only weak sensitivity to the driving force of the reactions. This insensitivity was tentatively interpreted as an indication that assembly of the reactant pairs into precursor complexes may be the step that limits the rate of the electron-transfer process.

The oxidation (or reduction) of a hydrophilic reactant dissolved in an aqueous solution by a hydrophobic coreactant dissolved in an organic solvent adjacent to, but immiscible with, the aqueous solution, can take place by means of electron transfer across the boundary separating the two phases. Discussions of the parameters that may affect the kinetics of such cross-phase electron-transfer reactions are reasonably abundant,¹ but experimental evaluation of reaction rates had been relatively sparse.² Recently, the application of new experimental techniques to measure the rates of cross-phase electron-transfer reactions has yielded a wider variety of experimental data.^{3–5} However, some of the data that have been reported are not in accord with expectations based on commonly espoused models of the interface between two immiscible liquids. For example, in a recent report from this laboratory, the rates of redox reactions occurring at the interface between nitrobenzene and water were observed to be insensitive to changes in the driving force of the reactions.^{4b} This insensitivity was exhibited both when the driving force for a fixed reactant pair was altered by changing the ionic compositions of the two adjoining phases as well as when the coreactants were varied to produce large differences in the formal redox potentials of the two reactants.^{4b}

The present experiments were carried out to obtain additional information about the rates of redox reactions between reactants residing in adjacent, immiscible phases. The effect of accompanying ion transfer on the rates of cross-phase electron-transfer was examined, as was the effect of changes in the potential differences at the liquid/liquid interface produced by changes in the ionic compositions of either liquid phase.

Experimental Section

Materials. Metalloporphyrins from Porphyrin Products, Inc. (Logan, UT) were purified by column chromatography on neutral alumina. Other chemicals and solvents were commercial products of high purity that were used as received. Cylindrical pyrolytic graphite electrodes with 0.32 cm² of the edges of the graphitic planes exposed (Union Carbide Co.) were mounted and pretreated as previously described.^{4a}

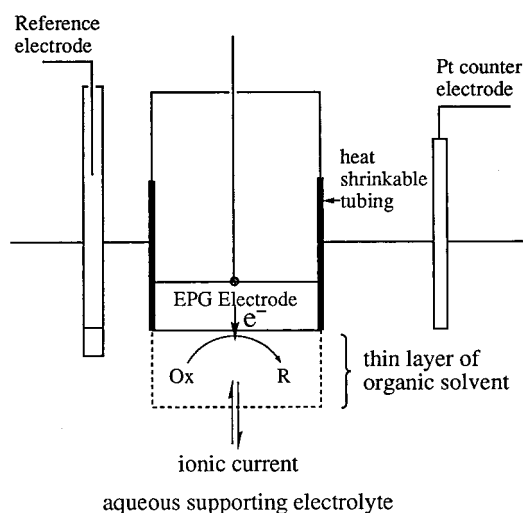


Figure 1. Schematic depiction of the electrochemical cell used to observe voltammetric responses from reactants dissolved in thin layers of organic solvents on graphite electrodes. The drawing is not to scale; the thickness of the thin layers employed was typically 25–50 μm .

Apparatus and Procedures. The electrochemical cells and instrumentation and the procedure employed for introducing thin layers of organic solvents on graphite electrode surfaces have been previously described.^{4a} A schematic depiction of the electrochemical cell employed is shown in Figure 1. The thicknesses of the layers of organic solvents were typically 20–30 μm . Supporting electrolytes and reactants were usually introduced into the organic solvents before the thin layers were placed on the electrode surfaces. When no supporting electrolyte was dissolved in the organic solvent used to form the thin layer, electrolyte from the aqueous solution that partitioned into the thin layer provided adequate conductance to avoid distortion in the voltammetric responses.

Results

Cyclic Voltammetry of Reactants Confined within Thin Layers of Organic Solvents. Before presenting the results of experiments designed to measure the rates of electron transfer

* Corresponding author. E-mail: fanson@cco.caltech.edu. Phone: (626) 395 6000. Fax: (626) 405 0454.

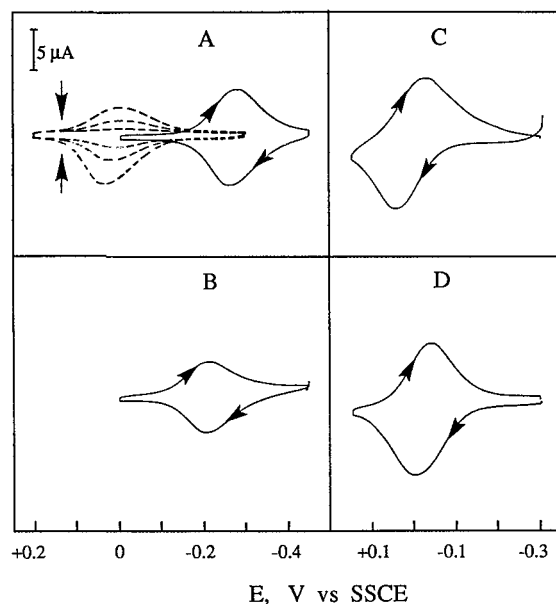


Figure 2. Cyclic voltammetry of the $\text{DMFc}^+/\text{DMFc}$ couple dissolved in thin layers of organic solvents in a cell like that shown in Figure 1: (A) $\sim 30\ \mu\text{m}$ thin layer of nitrobenzene containing 1.9 mM DMFc; (B) $\sim 30\ \mu\text{m}$ thin layer of 4-methylbenzonitrile containing 1.6 mM DMFc; (C) thin layer prepared from chloroform originally containing 0.8 mM DMFc; (D) thin layer prepared from benzene originally containing 0.9 mM DMFc. The rapid evaporation of the $4.0\ \mu\text{L}$ of solvent used to prepare the thin layers in (C) and (D) made their precise thicknesses and the concentrations of DMFc uncertain. The supporting electrolyte in the aqueous phase was 0.1 M NaClO_4 except for the dashed curves in (A), where 0.1 M tetraethylammonium bromide was used. In (A) and (B), the supporting electrolyte in the nonaqueous layer was provided by partitioning of the aqueous supporting electrolyte. In (C) and (D), 0.25 M $[\text{Hx}_4\text{N}]\text{ClO}_4$ was dissolved in the organic solvents before the thin layers were formed. Scan rate = $5\ \text{mV s}^{-1}$.

between reactants dissolved in adjoining, immiscible phases, voltammetric responses obtained with electroactive reactants present only in the organic thin layer were examined. Cyclic voltammetric responses from the $\text{DMFc}^+/\text{DMFc}$ couple (DMFc = decaethylferrocene) dissolved in thin layers prepared from four different immiscible organic solvents are shown in Figure 2. With the less volatile solvents, nitrobenzene and 4-methylbenzonitrile (Figure 2A,B), the thin layers were formed by transferring $1\ \mu\text{L}$ of the solvent to the electrode surface. The thickness of the resulting thin layer, ca. $30\ \mu\text{m}$, was smaller than the diffusion layer thickness at the low scan rate employed so that the voltammetric responses exhibited the symmetrical shapes and equal peak potentials expected under such circumstances.⁶ With the more volatile solvents, chloroform and benzene (Figure 2C,D), $3\text{--}4\ \mu\text{L}$ of the solvent were transferred to the electrode, and thicker layers resulted despite some evaporation of the solvents before the electrode was immersed in the aqueous phase. The resulting voltammetric responses (Figure 2C,D) were somewhat less symmetrical with greater separations between the peak potentials, as is expected when the thickness of the diffusion layer is smaller than that of the thin layer. With thin layers prepared from nitrobenzene and 4-methylbenzonitrile, NaClO_4 that partitioned from the aqueous into the nonaqueous phase constituted the supporting electrolyte in the organic phase. With benzene and chloroform layers it was necessary to dissolve a supporting electrolyte (tetra-*n*-hexylammonium perchlorate, $[\text{Hx}_4\text{N}]\text{ClO}_4$) in the organic phase before the thin layers were formed in order to obtain sufficient conductivity to avoid distortions in the voltammetric responses.

As long as the supporting electrolyte in the aqueous solution contained ClO_4^- anions, very little DMFc or DMFc^+ was lost from the organic layer as the potential of the EPG electrode was cycled to record the voltammograms in Figure 2. With supporting electrolytes composed of most other inorganic anions, DMFc^+ cations were lost from the thin layers during continuous cycling. For example, the dashed curves in Figure 2A show the diminishing responses obtained from the $\text{DMFc}^+/\text{DMFc}$ couple in a nitrobenzene (NB) thin layer when tetraethylammonium bromide was the supporting electrolyte in the aqueous (and nonaqueous) phase. The difference in the behavior obtained in these two supporting electrolytes is the result of the much less positive free energy of transfer from H_2O to NB of ClO_4^- than of Br^- and most other inorganic anions.^{1a,7} During the cycling of the electrode potential in experiments such as those in Figure 2, ionic current must cross the liquid/liquid interface in order to maintain electroneutrality within the nonaqueous layer. With supporting electrolytes containing ClO_4^- anions, much of this ionic current is carried by this anion, but with other anions, such as Br^- (dashed curves in Figure 2A), the quantity of supporting electrolyte that partitions from the aqueous phase into the NB layer is considerably less so that more of the ionic current must consist of DMFc^+ cations that cross from the thin layer of NB into the much more voluminous aqueous phase and are lost from the NB layer.

Differences in Potential Across the Aqueous/Nonaqueous Interface. When a uni-univalent salt such as $[\text{Et}_4\text{N}]\text{ClO}_4$, $[\text{Et}_4\text{N}]\text{Br}$ (Et_4N^+ = tetraethylammonium) or NaClO_4 is the only supporting electrolyte present in either phase, the difference in potential that develops at the interface between the aqueous and organic phases is expected to depend only on the standard ionic transfer potentials of the cationic and anionic components of the supporting electrolyte. In this case, the interfacial potential difference, $\Delta\phi_{\alpha\beta}$, was shown by Karpfen and Randles⁸ to be given by eq 1.

$$\Delta\phi_{\alpha\beta} = 0.5[(\Delta\phi_{\alpha\beta}^+) + (\Delta\phi_{\alpha\beta}^-)] \quad (1)$$

where $(\Delta\phi_{\alpha\beta}^+)$ and $(\Delta\phi_{\alpha\beta}^-)$ are the standard potentials for the transfer of the cation and anion, respectively, from phase α to phase β . These standard transfer potentials are independent of the concentrations of the ions so that $\Delta\phi_{\alpha\beta}$ should be independent of the quantity of supporting electrolyte present once its partitioning between the two phases has reached equilibrium. One consequence of this property is that the apparent formal potentials of redox couples dissolved in the organic phase, as measured with respect to a reference electrode in the aqueous phase, should not change if the concentration of the single, uni-univalent supporting electrolyte in the aqueous phase is changed. In Figure 3A (open circles) are shown formal potentials for the $\text{DMFc}^+/\text{DMFc}$ couple in thin layers of NB measured cyclic voltammetrically at several concentrations of $[\text{Et}_4\text{N}]\text{ClO}_4$ in the aqueous phase. The constancy of the measured formal potentials is in accord with expectations.⁹

In principle, invariant apparent formal potentials, as shown in Figure 3A with $[\text{Et}_4\text{N}]\text{ClO}_4$ as the supporting electrolyte, should be exhibited by all uni-univalent electrolytes.^{8,10,11} However, the partitioning of most inorganic ions into NB is so energetically unfavorable that it is difficult to obtain concentrations of such supporting electrolytes in NB that are large compared with redox couples whose formal potentials are of interest. For example, the NB thin layer used in Figure 2A, which was equilibrated with 0.1 M NaClO_4 in H_2O , contained only $16\ \mu\text{M}$ Na^+ and ClO_4^- ions based on the standard transfer potentials for these two ions.^{1a,7} Under these conditions, the

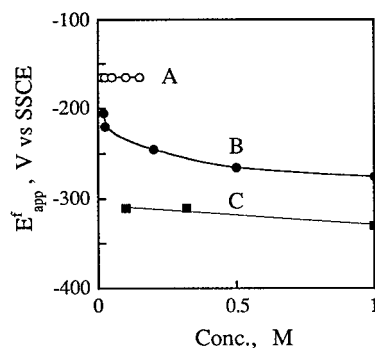


Figure 3. Effect of the concentration of supporting electrolyte in the aqueous solution on the apparent formal potentials of the $\text{DMFc}^+/\text{DMFc}$ couple in NB. Values of E_{app}^f were obtained from the average of the anodic and cathodic peak potentials of voltammograms such as the solid curve in Figure 2A. Supporting electrolyte: (A) $[\text{Et}_4\text{N}]\text{ClO}_4$, the range of concentrations examined was limited by the solubility of $[\text{Et}_4\text{N}]\text{ClO}_4$; (B) NaClO_4 , $[\text{DMFc}] = 1 \text{ mM}$; (C) NaClO_4 , $[\text{DMFc}] = 40 \mu\text{M}$. Differential pulse voltammetry was used to evaluate the formal potentials.

transfer of ions of the supporting electrolyte across the NB/ H_2O interface as the cyclic voltammograms used to evaluate the apparent formal potential of the $\text{DMFc}^+/\text{DMFc}$ couple are recorded produces a significant change in the ionic composition of the NB layer and, therefore, the potential difference at the NB/ H_2O interface. Thus, under such conditions, it is not surprising that adherence to eq 1 can break down, as shown by the data plotted in Figure 3B. (Changes in the ionic composition of the NB layer also occur during the recording of the cyclic voltammograms used to obtain the apparent formal potentials in Figure 3A, but these changes are relatively much smaller because of the much larger quantity of $[\text{Et}_4\text{N}]\text{ClO}_4$ than of NaClO_4 that spontaneously partitions into the NB layer.)

It follows from this explanation for the variations in the apparent formal potentials in Figure 3B that the magnitude of the variations should diminish if the concentration of the reactant in the NB layer is decreased because less supporting electrolyte would enter and leave the NB layer as the voltammograms were recorded. To test the utility of this approach, the experiments of Figure 3B were repeated with a thin layer containing only $40 \mu\text{M}$ $\text{DMFc} + \text{DMFc}^+$. Differential pulse¹² instead of cyclic voltammetry was used to evaluate the formal potentials because of the higher sensitivity of the differential pulse technique. As can be seen from the data in Figure 3C, decreasing the concentration of the reactant (DMFc) produced values of the apparent formal potentials that exhibited less variation with the concentration of the NaClO_4 supporting electrolyte. In addition, the difference of 0.17 V between the apparent formal potential in $[\text{Et}_4\text{N}]\text{ClO}_4$ supporting electrolytes (-0.16 V) and that in 1 M NaClO_4 (-0.33 V) is not far from the 0.21 V difference that can be calculated from eq 1 using tabulated values¹¹ of $(\Delta\phi_{\alpha}^{\beta})_+$ and $(\Delta\phi_{\alpha}^{\beta})_-$ for the two electrolytes.

Another way to overcome the complications that may be encountered when the concentration of supporting electrolyte that partitions into the organic phase is not much greater than the concentration of the reactant is to dissolve a hydrophobic supporting electrolyte in the organic phase. This tactic produces values of $\Delta\phi_{\alpha}^{\beta}$ with magnitudes that can be calculated from equations more complex than eq 1.^{10,11,13} In some cases, the values of $\Delta\phi_{\alpha}^{\beta}$ are essentially unaffected by the addition of a second electrolyte to the nonaqueous phase. For example, with 0.1 M $[\text{Et}_4\text{N}]\text{ClO}_4$ in the aqueous phase, the partitioning of this salt between the two phases controls the potential difference between them. Addition of a nonpartitioning hydrophobic

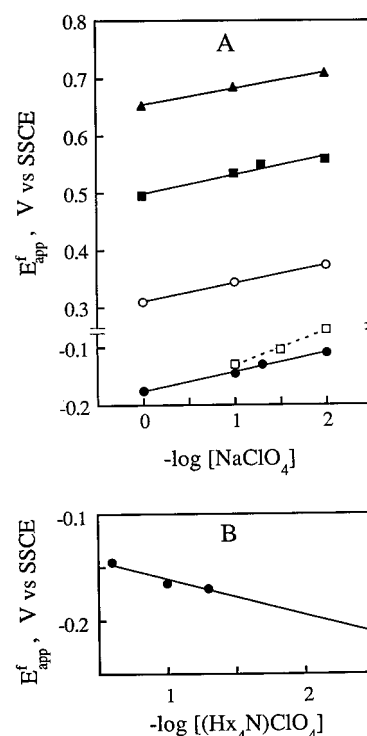


Figure 4. (A) Apparent formal potentials of redox couples dissolved in thin layers of NB also containing 0.25 M $[\text{Hx}_4\text{N}]\text{ClO}_4$. The concentration of NaClO_4 in the aqueous phase was varied. Redox couples and their concentrations: (\blacktriangle) 1.2 mM $\text{ZnTPP}^+/\text{ZnTPP}$; (\blacksquare) 1.4 mM $\text{CoTPP}^+/\text{CoTPP}$ (CoTPP = cobalt tetraphenylporphyrin); (\circ) 0.7 mM $\text{VO}(\text{salen})^+/\text{VO}(\text{salen})$ ($\text{H}_2 \text{ salen}$ = N,N' -ethylenebis(salicylideneamine)); (\bullet) 1.2 mM $\text{DMFc}^+/\text{DMFc}$; (\square) 1.2 mM $\text{DMFc}^+/\text{DMFc}$ in 15 mL of NB overlaid with 20 mL of the aqueous phase. (B) 1.2 mM $\text{ZnTPP}^+/\text{ZnTPP}$, but the aqueous phase contained 0.1 M NaClO_4 and the concentration of $[\text{Hx}_4\text{N}]\text{ClO}_4$ in the NB layer was varied. All values of E_{app}^f were evaluated from cyclic voltammograms such as those in parts A and B of Figure 2.

electrolyte to the nonaqueous phase causes essentially no change in $\Delta\phi_{\alpha}^{\beta}$. Thus, the formal potentials measured for the $\text{DMFc}^+/\text{DMFc}$ couple in NB from voltammograms such as that in Figure 2A do not change when even 0.25 M $[\text{Hx}_4\text{N}]\text{ClO}_4$ is dissolved in the NB phase. However, when the supporting electrolyte in the aqueous phase is largely excluded from the nonaqueous phase, e.g., NaClO_4 , and a hydrophobic salt is present in the nonaqueous phase, e.g., $[\text{Hx}_4\text{N}]\text{ClO}_4$, the value of $\Delta\phi_{\alpha}^{\beta}$ may change with the concentration of either supporting electrolyte. The rate of change of the interfacial potential depends on the nature of the two immiscible solvents used to form the interface, on the identities and concentrations of the electrolytes dissolved in each solvent,^{10,11,13} and on the ratio of the volumes of the two phases.¹⁴ The dependence on the volume ratio becomes particularly important when one of the phases is a thin layer as in the present experiments. Apparent formal potentials for several redox couples dissolved in thin layers of NB, which also contained 0.25 M $[\text{Hx}_4\text{N}]\text{ClO}_4$, were measured as the concentration of NaClO_4 in the adjacent aqueous phase was changed. The results are shown in Figure 4A. Shown in Figure 4B are the changes in the apparent formal potential of the $\text{ZnTPP}^+/\text{ZnTPP}$ redox couple (ZnTPP = zinc tetraphenylporphyrin) that resulted when the concentration of $[\text{Hx}_4\text{N}]\text{ClO}_4$ in the NB thin layer was varied with a fixed concentration of NaClO_4 in the aqueous phase. One expects slopes near 60 mV per decade for plots such as those in Figure 4 when the volumes of the two equilibrating phases are comparable,^{10,11,13} and just such behavior was reported by Tsionsky et al.^{3b} for the $\text{ZnTPP}^+/\text{ZnTPP}$

ZnTPP couple when the interface was formed between comparable volumes of benzene and water. However, in the present experiments with thin layers of NB, the ratio of the volume of the organic to the aqueous phase was typically 5×10^{-5} . Kakiuchi¹⁴ has shown that under such conditions the slopes of plots such as those in Figure 4A should be 30 mV per decade. All of the solid-line plots in Figure 4 have slopes in the range of 30–34 mV per decade. Thus, these data provide a clear verification of the theoretical analysis given by Kakiuchi.¹⁴

Confirmation of this conclusion was obtained by repeating the measurements of formal potentials using comparable volumes of NB and water layered vertically in an electrochemical cell. A graphite electrode was placed in the lower, NB phase and the reference and auxiliary electrodes were in the upper, aqueous phase. Apparent formal potentials of the DMFc⁺/DMFc couple in the NB phase measured with this experimental arrangement are shown in the dashed plot in Figure 4A. The slope is 50 mV per decade, a value which is in fair agreement with the 59 mV per decade expected.^{10,11,13,14}

The utility of data like those in Figure 4A is the access they provide to individual values of $\Delta\phi_{\alpha}^{\beta}$ at liquid/liquid interfaces in thin layer experiments. These values are important because the magnitude of $\Delta\phi_{\alpha}^{\beta}$ is expected to influence the rate of charge-transfer across the interface,^{1,3} although Schmickler has argued that changes in $\Delta\phi_{\alpha}^{\beta}$ may affect reaction rates only weakly.¹⁵

Electron Transfer between Reactants in Adjoining Liquid Phases. When redox-active reactants are present in the aqueous solution beneath the thin layers of organic solvent in cells such as the one shown in Figure 1, electron-transfer between co-reactants located in the two phases can occur and the reaction rate can be monitored electrochemically. A typical experimental arrangement that can be used for the measurement of cross-phase reaction rates^{4b} is shown in the Supporting Information. The thin layer of organic solvent prevents hydrophilic reactants dissolved in the aqueous phase from reaching the electrode surface to be directly oxidized or reduced. However, hydrophobic reactants dissolved in the thin layer of organic solvent can be oxidized or reduced at the electrode surface and diffuse to the liquid/liquid interface where a redox reaction with reactants in the aqueous phase may occur. With appropriate choices of the reactant concentrations in the two phases, a steady-state is established and the magnitude of the steady-state current that flows through the thin layer of organic solvent to the underlying electrode can be analyzed to evaluate the rate of the cross-phase redox reaction. For example, shown in Figure 5 is a set of the current–potential responses obtained with an experimental arrangement like the one shown in the Supporting Information with $\text{Ru}(\text{NH}_3)_6^{3+}$ present in the aqueous phase. Before the thin layer of organic solvent was placed on the surface of the graphite electrode, the usual, reversible cyclic voltammetric response of the $\text{Ru}(\text{NH}_3)_6^{3+/2+}$ couple was observed (Figure 5A). After a thin layer of nitrobenzene was placed on the electrode surface to separate it from the aqueous solution, no voltammetric current was observed for the reduction of $\text{Ru}(\text{NH}_3)_6^{3+}$ because this cation could no longer reach the electrode surface (Figure 5B).

When DMFc⁺ was added to the thin layer of NB, a cathodic current was obtained (Figure 5D) at the potential where DMFc⁺ is reduced to DMFc (Figure 5C). The current rose to a cathodic plateau corresponding to a pseudosteady state in which the concentration of $\text{Ru}(\text{NH}_3)_6^{3+}$ at the $\text{H}_2\text{O}/\text{NB}$ interface was essentially constant (equal to its value in the bulk of the aqueous phase) and the concentration gradient of DMFc in the NB layer

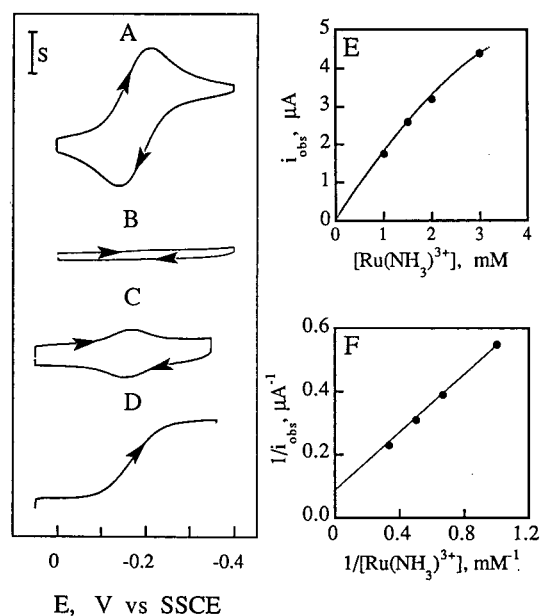


Figure 5. Voltammetric responses obtained with a cell like the one shown in Figure S1 (Supporting Information). (A) Cyclic voltammetry of 0.5 mM $\text{Ru}(\text{NH}_3)_6^{3+}$ at the EPG electrode before a thin layer of NB was introduced. Supporting electrolyte: 0.08 M $[\text{Et}_4\text{N}]\text{ClO}_4$. Scan rate = 5 mV s⁻¹. *S* = 5 μA. (B) Repeat of (A) after the electrode was covered with a 30 μm layer of NB. (C) Cyclic voltammetry of 0.20 mM DMFc dissolved in the NB thin layer. The aqueous phase contained only supporting electrolyte (0.08 M $[\text{Et}_4\text{N}]\text{ClO}_4$). *S* = 2 μA. (D) Repeat of (C) with 2.0 mM $\text{Ru}(\text{NH}_3)_6^{3+}$ added to the aqueous phase. *S* = 2 μA. (E) Variation of the steady-state currents such as that in (D), *i*_{obs}, with the concentration of $\text{Ru}(\text{NH}_3)_6^{3+}$ in the aqueous phases. (F) Reciprocal plot of data from (E).

became linear with a magnitude that was determined by the rate at which the DMFc reduced $\text{Ru}(\text{NH}_3)_6^{3+}$ at the $\text{H}_2\text{O}/\text{NB}$ interface.

The observed plateau current in curves such as that in Figure 5D, *i*_{obs}, is expected to obey eq 2^{4b,16}

$$\frac{1}{i_{\text{obs}}} = \frac{1}{i_{\text{D}}} + \frac{1}{i_{\text{k}}} \quad (2)$$

where *i*_D measures the rate of the diffusion-limited transport of the reactant (DMFc) in the NB layer,

$$i_{\text{D}} = \frac{nFAC_{\text{NB}}D}{\delta} \quad (3)$$

where *n* is the number of electrons involved in the electrode reaction, *F* is Faraday's constant, *A* is the electrode area, *C*_{NB} and *D* are the concentration and diffusion coefficient of the reactant in the NB layer, respectively, and δ is the thickness of the thin layer. *i*_k in eq 2 is the kinetic current that measures the rate of the (assumed) first-order reaction between the reactants in the two phases,

$$i_{\text{k}} = nFAkC_{\text{NB}}C_{\text{H}_2\text{O}} \quad (4)$$

where *k* is a bimolecular rate constant (with units of cm s⁻¹ M⁻¹), *C*_{H₂O} is the concentration of the reactant in the aqueous phase, and the other terms have been defined. Values of *i*_{obs} measured at several concentrations of $\text{Ru}(\text{NH}_3)_6^{3+}$ are plotted in Figure 5E. The nonlinear plot is expected on the basis of eq 2. At sufficiently high concentrations of $\text{Ru}(\text{NH}_3)_6^{3+}$, *i*_{obs} would become independent of this concentration because the current would be limited by the diffusion of DMFc across the thin layer

TABLE 1: Apparent Bimolecular Rate Constants for Electron Transfer between Pairs of Redox Reactants in Adjoining NB/H₂O Phases^a

reactant in H ₂ O ^b	$E_{\text{H}_2\text{O}}^{\text{f}}$ mV	reactant in NB ^d	E_{NB}^{f} mV	ΔE^{f} mV	k , cm s ⁻¹ M ⁻¹
Fe(CN) ₆ ³⁻	185	DMFc	-145	330	0.9
Ru(CN) ₆ ⁴⁻	750	ZnTPP ⁺	690	-60	0.8
Mo(CN) ₈ ⁴⁻	551	ZnTPP ⁺	690	139	1.7
Fe(CN) ₆ ⁴⁻	185	ZnTPP ⁺	690	505	1.8
Ru(NH ₃) ₆ ³⁺	-170	DMFc	-165	-5	0.3 ^g
IrCl ₆ ²⁻	715	Fc	185	530	1.4

^a Data from ref 4b except as noted. ^b Supporting electrolyte 0.1 M NaClO₄ + 0.1 M NaCl except 0.1 M [Et₄N]ClO₄ with Ru(NH₃)₆³⁺ and 2 M HClO₄ with IrCl₆²⁻. ^c Formal potential of the reactant couple in the aqueous phase vs a sodium chloride saturated calomel reference electrode (SSCE) in the aqueous phase. ^d Supporting electrolyte 0.25 M [H₄N]ClO₄ except [Et₄N]ClO₄ with Ru(NH₃)₆³⁺ and HClO₄ with IrCl₆²⁻. ^e Formal potential of the reactant couple in the NB phase vs SSCE (aqueous). ^f Driving force of the redox reaction. ^g This work.

of NB.^{4b} This condition could not be reached in the present experiment because of the limited solubility of Ru(NH₃)₆³⁺ in [Et₄N]ClO₄.

Steady-state plateau currents such as that in Figure 5D are obtained when the concentration of the reactant in the aqueous phase remains essentially constant at the NB/H₂O interface during the time involved in the measurement of the plateau current. The ratio of the concentration of the aqueous phase reactant at the interface to that in the bulk of the solution can be estimated as $(1 - (t/\tau)^{1/2})$ where t is the experimental measurement time and τ is the (chronopotentiometric) transition time¹⁷ corresponding to the observed, steady-state current. Thus, for the reactant concentration at the interface to remain within, say, 80% of its value in the bulk of the solution, $(t/\tau)^{1/2} < 0.2$ so that, for typical measurement times of ~ 10 s, $\tau > 2.5 \times 10^2$ s. With the experimental parameters in the present experiments, i.e., $A = 0.32$ cm², $D \approx 6 \times 10^{-6}$ cm² s⁻¹, it follows from the Sand equation¹⁷ that the interfacial concentration of the aqueous phase reactant will be decreased by less than 20% when the ratio of the steady-state current to the bulk concentration of the reactant, $i_{\text{obs}}/C_{\text{H}_2\text{O}}$, is less than ~ 4 μA (mM)⁻¹. This condition was fulfilled in all of the experiments used to evaluate the rate constants in Table 1.

It follows from eqs 2–4 that a plot of $(i_{\text{obs}})^{-1}$ vs $(C_{\text{H}_2\text{O}})^{-1}$ should be linear with a slope that can be used to calculate k and a reciprocal intercept that corresponds to the limiting value of i_{D} that should be obtained at sufficiently high values of $C_{\text{H}_2\text{O}}$. Such a reciprocal plot is shown in Figure 5F. A value of $k = 0.32$ cm s⁻¹ M⁻¹ can be calculated from the slope of the plot. The reciprocal intercept of 11 μA is in reasonable agreement with the value of i_{D} (12 μA) that can be calculated from eq 3 and the known values of $D = 6 \times 10^{-6}$ cm² s⁻¹ and $\delta = 30$ μm .

Dependence of k on Ionic Strength. The rate of electron transfer between reactants in adjoining immiscible liquid layers is expected to be affected, at least to some extent,¹⁵ by the potential difference that exists across the liquid/liquid interface.^{1,3} As was pointed out above in connection with eq 1, when the same uni-univalent supporting electrolyte is present in both phases, the potential drop across the interface does not change with the ionic strength of the supporting electrolyte.⁸ By taking advantage of this property, it is possible to examine the effects of changes in the concentration of supporting electrolyte on the rate of electron-transfer reactions while maintaining a constant value of the interfacial potential difference. Thus, one can investigate the possibility that specific ionic interactions between

reactants and supporting electrolytes affect reaction rates, and, under non-steady-state conditions, one can determine whether the rate of transfer of ions of the supporting electrolyte across the liquid/liquid interface affects the rate of cross-phase electron-transfer reactions. For example, experiments such as those shown in Figure 5 were repeated with two different concentrations of [Et₄N]ClO₄ in the aqueous phase, 0.01 and 0.08 M. The reciprocal plots were similar to the plot in Figure 5F with slopes that corresponded to $k = 0.29$ and 0.34 cm s⁻¹ M⁻¹. These results indicated that association between Ru(NH₃)₆³⁺ and ClO₄⁻ ions in the aqueous phase, if any, did not influence the rate of reduction of Ru(NH₃)₆³⁺ by DMCf in the NB phase.

Electron Transfer with Ion Transfer. The steady-state currents that are measured in experiments such as those in Figure 5D involve only the transfer of electrons across the electrode/NB and NB/H₂O interfaces. No ion transfer accompanies the electron transfer at steady-state. However, in most previous evaluations of the rates of redox reactions at liquid/liquid interfaces, ion transfer across the interfaces was coupled to the electron transfer in order to maintain electroneutrality within the two phases.^{2,3} The rates of cross-phase ion transfer are typically rapid, diffusion-controlled processes which would not be expected to impede the rate of cross-phase electron transfer reactions.^{1f} Nevertheless, it seemed worthwhile to test this expectation by comparing the rate of a cross-phase redox reaction proceeding in the presence of accompanying ion-transfer with the rate of the same reaction under steady-state conditions where no ion transfer occurred. For the cross-phase reaction between [Ru(NH₃)₆³⁺]_{H₂O} and (DMFc)_{NB}, a rate constant of 0.32 cm s⁻¹ M⁻¹ was obtained in the absence of ion transfer (Figure 5F). To evaluate the rate of the same reaction in the presence of ion transfer, an experiment was performed with the electrode at open circuit using the experimental arrangement depicted in Figure 6A. The DMCf in the NB thin layer was first converted into its reduced form by maintaining the EPG electrode at -0.35 V for ca. 10 s. (During this period, the concentration of Ru(NH₃)₆³⁺ at the NB/H₂O interface was not significantly diminished from its relatively high value in the bulk of the aqueous phase because of the low rate of the redox reaction.) The EPG electrode was then abruptly placed at open circuit, and its potential was recorded as the DMCf in the NB thin layer was oxidized to DMCf⁺ by reaction with Ru(NH₃)₆³⁺ at the NB/H₂O interface (Figure 6B). The experimental measurement times were longer than the time required for the DMCf to diffuse across the 30 μm layer of NB (~ 0.5 s) so that the concentrations of DMCf and DMCf⁺ were assumed to remain uniform within the thin layer and were calculated at any time from the observed electrode potential using the Nernst equation. A first-order plot of $\log[\text{DMFc}]$ vs time was prepared (Figure 6C), and the rate constant for the cross-phase redox reaction was evaluated from the slope of the resulting linear plot using eq 5

$$k = \frac{-2.303(\text{slope})\delta}{C_{\text{H}_2\text{O}}} \quad (5)$$

The value of k obtained from Figure 6C was 0.2 cm s⁻¹ M⁻¹. (The deviation of the points at longer times from the line in Figure 6C is probably a reflection of the fact that an intrinsically reversible reaction was analyzed as if it were irreversible.) The value of k obtained from the slope of the line in Figure 6C is not significantly different from the 0.32 cm s⁻¹ M⁻¹ obtained when the experiments were carried out under steady-state conditions (Figure 5) from which it may be concluded that, as

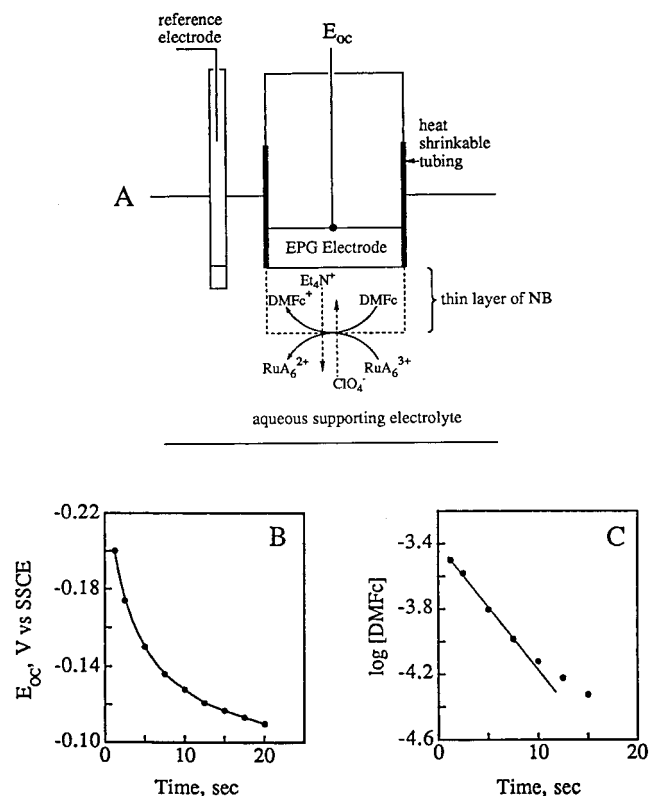


Figure 6. (A) Schematic depiction of the experimental arrangement used to measure the rate of cross-phase redox reactions accompanied by cross-phase ion transfer. The initial oxidation state of the DMFc/DMFc⁺ couple (0.44 mM) in the NB thin layer was adjusted by imposing an initial potential on the EPG electrode. (B) The potential of the electrode at open circuit after it was abruptly disconnected from the potentiostat. (C) First-order kinetic plot of the concentration of DMFc in the NB thin layer as calculated from the Nernst equation and the potentials in (B).

expected, ion transfer across the NB/H₂O interface that occurred during the experiments in Figure 6 did not affect the rate of the cross-phase redox reaction.

Discussion

Concentration Dependences of $\Delta\phi_{\alpha\beta}$. The use of simple cyclic voltammetric measurements of apparent formal potentials for reactants confined with thin layers of organic solvents to monitor changes in the potential differences, $\Delta\phi_{\alpha\beta}$, existing at liquid/liquid interfaces is an attractive feature of the thin layer technique. However, as the results shown in Figure 3B demonstrate, difficulties can be encountered when the reactant concentrations in the thin layer are comparable to or greater than the concentration of supporting electrolyte. The use of low reactant concentrations and electrochemical techniques with higher sensitivities than cyclic voltammetry is one way to overcome this difficulty, as was demonstrated in Figure 3C.

The changes in $\Delta\phi_{\alpha\beta}$ that can be inferred from the changes in E_{app}^f values in Figure 4 matched the 30 mV per decade predicted by Kakiuchi.¹⁴ This confirmation of his analysis shows that data from thin layer experiments can be utilized with confidence.

Electron-Transfer Not Rate Determining. The experimental demonstration via Figures 5 and 6 that the rate of transfer of the ions comprising the supporting electrolyte across the NB/H₂O interface does not limit the rate of the cross-phase redox reaction was the anticipated result. However, the presently available data do not support the conclusion that simple electron-

transfer between the coreactants located in the separated phases is the process which controls the magnitudes of the steady-state currents (and the bimolecular rate constants evaluated from them) in experiments such as those in Figure 5. In Table 1 is collected a set of rate constants obtained for a variety of phase-separated, redox coreactants. The free energy changes for the various electron-transfer reactions vary by over 500 mV. Despite this large variation in driving force, the rate constants obtained for the various reactions differ by less than an order of magnitude. Differences in self-exchange rates among the reactant pairs are not large enough to explain this apparent insensitivity of the rates of the redox reactions to their equilibrium constants.

Attribution of this insensitivity to a mechanism in which one of the coreactants partitioned into the phase containing the other reactant prior to electron transfer between the two in the same phase is also unsatisfactory because the equilibrium partitioning into NB of say, Fe(CN)₆⁴⁻ or Ru(CN)₆⁴⁻, is unlikely to be sufficiently different to compensate for the large difference in the equilibrium constants for the oxidation of these two ions by ZnTPP⁺ (Table 1).

The presently available results for the NB/H₂O interface might be rationalized by appealing to the likely diffuse nature of the region separating the pure (or mutually saturated) phases, as pointed out by Schmickler.^{1f,10} The formation of precursor complexes within this interfacial region,¹⁸ which would require both reactants to enter a medium against a partitioning barrier favoring their exclusion, could constitute a rate-determining step which would be influenced very little by the driving force for the subsequent, faster, electron-transfer step. Experiments to test this speculation by examining a wider range of coreactants would be desirable and are presently underway.

Comparisons of Rate Constants. It would be of interest to compare the bimolecular rate constants (cm s⁻¹ M⁻¹) for the reactant pairs in Table 1 with the corresponding heterogeneous rate constants (cm s⁻¹) and the homogeneous self-exchange rate constants (M⁻¹ s⁻¹) for each individual redox couple. The relationships among these three types of rate constants, as discussed by Marcus,¹⁹ are such that only products of the heterogeneous or homogeneous self-exchange constants could be calculated from the measured value of the bimolecular rate constants in Table 1. However, such calculations would suffer from uncertainties about how the observed reaction rates should be corrected to correspond to those expected when the driving force, ΔE , is 0 mV.

At benzene/water interfaces, behavior in accord with the Marcus treatment of driving force dependences was reported for a few reactions by Bard and co-workers.^{3c} However, as reported previously^{4b} (and shown in Table 1), at the NB/water interface some of the same reactant pairs exhibit rates with a much smaller sensitivity to driving force than those predicted by the Marcus equations.¹⁹ The origin of the differences in the behaviors observed for the two interfaces remains to be fully understood, but possible differences in their sharpness may be a contributing factor. Until data are available for a broader set of reactant pairs and liquid/liquid interfaces, it seems premature to attempt to compare the values of bimolecular rate constants such as those in Table 1 with their more familiar counterparts at electrode surfaces and in homogeneous solutions.

Conclusions

Recently introduced methodology for the separation of an electrode surface from an aqueous solution by a thin, adherent layer of an immiscible solvent⁴ has facilitated the measurement

of rates of electron transfer across liquid/liquid interfaces. The paucity of previous experimental data on such processes has impeded the development and testing of proposals as to how the structure and composition of liquid/liquid interfaces affects the electron-transfer rates. The experiment results described in this report have highlighted some of the complications that can attend even the simplest of electron-transfer reactions when the reactant pair are separated by a liquid/liquid interface. The results serve to support Schmickler's assessment^{1f} that electron transfer reactions across liquid/liquid interfaces are inherently more complex to analyze than are reactions at typical electrode/solution interfaces.

Acknowledgment. This work was supported by the National Science Foundation. Helpful discussions with Dr. Stephen Feldberg are a pleasure to acknowledge. We are grateful to a reviewer for calling our attention to reference 14.

Supporting Information Available: A figure depicting the cell and experimental arrangement utilized in the evaluation of the rates of cross-phase redox reactions. This material is available free of charge via the Internet at <http://pubs.acs.org>.

References and Notes

- (1) (a) Girault, H. H.; Schiffrin, D. J. *Electroanalytical Chemistry*; Bard, A. J., Ed.; Marcel Dekker: New York, 1989; Vol. 15, p 1. (b) Girault, H. H.; *Modern Aspects of Electrochemistry*; Bockris, J. O'M., Conway, B. E., White, R. E., Eds.; Plenum Press: New York, 1993; Vol. 25, p 1. (c) Marcus, R. A. *J. Phys. Chem.* **1990**, *94*, 1050, 4155, 7742. (d) Marcus, R. A. *J. Phys. Chem.* **1991**, *95*, 2010. (e) Marcus, R. A. *J. Phys. Chem.* **1995**, *99*, 5742. (f) Schmickler, W. *Interfacial Electrochemistry*; Oxford University Press: New York, 1996; Chapter 12. (g) Quinn, B.; Lahtinen, R.; Murtomäki, L.; Kontturi, K. *Electrochim. Acta* **1998**, *44*, 47.
- (2) (a) Geblewicz, G.; Schiffrin, D. J. *J. Electroanal. Chem.* **1988**, *244*, 27. (b) Cunnane, V. J.; Schiffrin, D. J.; Beltran, C.; Geblewicz, G.; Solomon, T. *J. Electroanal. Chem.* **1988**, *247*, 203. (c) Cheng, Y.; Schiffrin, D. J. *J. Electroanal. Chem.* **1991**, *319*, 153. (d) Cheng, Y.; Schiffrin, D. J. *J. Chem. Soc., Faraday Trans.* **1994**, *90*, 2517.
- (3) (a) Wei, C.; Bard, A. J.; Mirkin, M. V. *J. Phys. Chem.* **1995**, *99*, 16033. (b) Tsionsky, M.; Bard, A. J.; Mirkin, M. V. *J. Phys. Chem.* **1996**, *100*, 17881. (c) Tsionsky, M.; Bard, A. J.; Mirkin, M. V. *J. Am. Chem. Soc.* **1997**, *119*, 10785. (d) Delville, M.-H.; Tsionsky, M.; Bard, A. J. *Langmuir* **1998**, *14*, 2774.
- (4) (a) Shi, C.; Anson, F. C. *Anal. Chem.* **1998**, *70*, 3114. (b) Shi, C.; Anson, F. C. *J. Phys. Chem.* **1998**, *49*, 9850.
- (5) Ding, Z.; Fermin, D. J.; Brevet, P.-F.; Girault, H. H. *J. Electroanal. Chem.* **1998**, *458*, 139.
- (6) Bard, A. J.; Faulkner, L. R. *Electrochemical Methods*; Wiley: New York, 1980; p 410.
- (7) Danil de Namor, A. F.; Hill, T.; Sigstad, E. *J. Chem. Soc., Faraday Trans.* **1983**, *79*, 2713.
- (8) Karpfen, F. M.; Randles, J. E. B. *Trans. Faraday Soc.* **1953**, *49*, 823.
- (9) The measured apparent formal potentials would, of course, be affected by any changes in the junction potential at the reference electrode/aqueous phase interface as the concentration of supporting electrolyte in the aqueous phase was changed. However, such changes were demonstrated to be negligible in the present experiments by showing that the formal potential of reversible redox couples, e.g., $\text{Ru}(\text{NH}_3)_6^{3+/2+}$, dissolved in the aqueous phase and measured at a bare graphite electrode, did not change significantly with the concentration of the supporting electrolyte in the aqueous phase.
- (10) Markin, V. S.; Volkov, A. G. *J. Colloid Interface Sci.* **1989**, *131*, 382.
- (11) Volkov, A. G.; Deamer, D. W.; Tanelian, D. L.; Markin, V. S. *Liquid Interfaces in Chemistry and Biology*; Wiley: New York, 1998; Chapter 4. (Note the typographical error in eq 4.41: the coefficient of the second term on the rhs should be RT/F instead of $RT/2F$.)
- (12) Reference 6, p 190.
- (13) (a) Hung, L. Q. *J. Electroanal. Chem.* **1980**, *115*, 159. (b) Hung, L. Q. *J. Electroanal. Chem.* **1983**, *149*, 1.
- (14) Kakiuchi, T. *Anal. Chem.* **1996**, *68*, 3658.
- (15) Schmickler, W. *J. Electroanal. Chem.* **1997**, *428*, 123.
- (16) Andrieux, C. P.; Savéant, J.-M. *Molecular Design of Surfaces*; Murray, R. W., Ed.; Wiley: New York, 1992.
- (17) Reference 6, pp 253–254.
- (18) Girault, H. H. J.; Schiffrin, D. J. *J. Electroanal. Chem.* **1988**, *244*, 15.
- (19) (a) Marcus, R. A. *J. Phys. Chem.* **1990**, *94*, 4152; (correction) **1990**, *94*, 7742. (b) Marcus, R. A. *J. Phys. Chem.* **1991**, *95*, 2010; (correction) **1995**, *99*, 5742.